

Nonlinear evolution of parallel propagating Alfvén waves: Vlasov - MHD simulation

Nariyuki, Y.^a, Umeda, T.^b, Kumashiro, T.^c, Hada, T.^c

^a*Department of Electrical Engineering and Information Science, Kochi National College of Technology, Kochi 783-8508, Japan*

^b*Solar-Terrestrial Environment Laboratory, Nagoya University, Nagoya, Aichi 464-8601, Japan*

^c*E.S.S.T., Kyushu University, 6-1, Kasuga-koen, Kasuga City, Fukuoka 816-8580, Japan*

Abstract

Nonlinear evolution of circularly polarized Alfvén waves are discussed by using the recently developed Vlasov-MHD code, which is a generalized Landau-fluid model. The numerical results indicate that as far as the nonlinearity in the system is not so large, the Vlasov-MHD model can validly solve time evolution of the Alfvénic turbulence both in the linear and nonlinear stages. The present Vlasov-MHD model is proper to discuss the solar coronal heating and solar wind acceleration by Alfvén waves propagating from the photosphere.

Key words: solar wind, Alfvén waves, Vlasov simulation

1. Introduction

2 Large-amplitude Alfvénic fluctuations are ubiquitous in the heliosphere,
 3 especially in the fast solar wind (Bruno and Carbone, 2005). Nonlinear evo-
 4 lution and dissipation of these fluctuations are thought to play important
 5 roles in heating of the solar wind plasmas (Suzuki and Inutsuka, 2006; Wu
 6 and Yoon, 2007; Araneda *et. al.*, 2008; Valentini *et. al.*, 2008) and gener-
 7 ation of the localized structures (Tsurutani *et. al.*, 2005; Vasquez *et. al.*,
 8 2007; Lin *et. al.*, 2009). Since these fluctuations are typically robust for lin-
 9 ear ion-cyclotron damping due to their small wave frequencies and for linear
 10 Landau damping due to their small propagation angle relative to the back-
 11 ground magnetic field, wave-wave interactions (parametric instabilities) are
 12 significant processes of their nonlinear evolution.

13 The quasi-parallel propagating Alfvénic fluctuations can resonate with
14 both the parallel and obliquely propagating magnetohydrodynamic (MHD)
15 waves (Mjølhus and Hada, 1990; Champoux *et. al.*, 1999; Nariyuki *et. al.*,
16 2008). In uniform plasmas with a typical parameter of the solar wind, parallel
17 propagating Alfvén waves dominantly resonate with the parallel propagating
18 Alfvén waves and ion acoustic waves. It is important that Alfvénic fluctua-
19 tions can resonate with the “kinetic” wave modes such as ion acoustic waves.
20 Namely, even if the fluid approximation is valid for Alfvénic fluctuations
21 themselves, the ion kinetics should be considered for parametric instabili-
22 ties (Araneda, 1998; Bugnon *et. al.*, 2004; Nariyuki and Hada, 2006; 2007,
23 Araneda *et. al.*, 2007).

24 Furthermore, in the plasmas with inhomogeneity and/or unstable velocity
25 distribution functions such as beam components, the resonance and dissipa-
26 tion processes can be different from those in the homogenous plasmas
27 (Tsikrauri *et. al.*, 2005; Suzuki and Inutsuka, 2005; 2006; Wang *et. al.*,
28 2006; Suzuki, 2008; Nariyuki *et. al.*, 2009). The kinetic Alfvén waves which
29 propagate at oblique angles relative to the background magnetic field can be
30 excited by the proton beams in the solar wind (Daughton and Gary, 1998;
31 Yin *et. al.*, 2007). We note that such beam-excited waves can preferentially
32 interact with the finite-amplitude parallel propagating Alfvén waves. Actu-
33 ally, the observational studies imply the importance of the kinetic Alfvén
34 waves on the dissipation of the Alfvénic turbulence (Leamon *et. al.*, 1998;
35 Hamilton *et. al.*, 2008).

36 As mentioned above, the nonlinear evolution and dissipation processes
37 of Alfvénic fluctuations in the solar wind are *cross scale coupling processes*,
38 in which the MHD-, ion-, and electron-scale phenomena coexist and mutu-
39 ally interact. Moreover, it is worth noting that the heating and acceleration
40 process of plasmas by Alfvénic fluctuations are desired to be slot into the he-
41 liospheric global simulation models (*e.g.*, Nakamizo *et. al.*, 2009). Thus, the
42 development of the alternative “kinetic” MHD models, which are the “mid-
43 del scale” model including some non-MHD effects, is necessary for *systematic*
44 understanding on such cross scale coupling processes.

45 As one of such models, we have recently developed a new Vlasov simu-
46 lation code named Vlasov-MHD code (1-D in the configuration space, 1-D
47 in “kinetic ” velocity space, and 2-D in “MHD ” velocity space), in order
48 to study basic properties of nonlinear evolution of Alfvén waves (Kumashiro
49 *et. al.*, 2009). The concept of the Vlasov- MHD model is the generalized
50 model of the so-called Landau fluid model (Passot and Sulem, 2003; Bugnon

51 *et. al.*, 2004), which includes the nonlinear wave-particle interactions. The
 52 linear analysis of the Vlasov-MHD model has been carried out (Araneda,
 53 1998; Nariyuki and Hada, 2006; 2007, Araneda *et. al.*, 2007) and has con-
 54 cluded that as far as the amplitude of the parent waves is not so large, the
 55 growth rates of the linear analysis are consistent with those in the numer-
 56 ical results of the ion hybrid simulation. Kumashiro *et. al.*(2009) performed
 57 the numerical simulation using the Vlasov-MHD code with the Hall-effect
 58 (Vlasov-Hall-MHD code) and demonstrated that the linear growth of para-
 59 metric instabilities of Alfvén waves are almost consistent with those of the
 60 ion hybrid simulation.

61 In the present paper, we discuss the nonlinear evolution of Alfvén waves
 62 using the Vlasov-Hall-MHD code. In section 2, we briefly introduce the
 63 numerical schemes of Vlasov-Hall-MHD code. We present the simulation
 64 results in section 3. Section 4 summarizes the results and briefly discuss the
 65 future issues.

66 2. Vlasov-Hall-MHD code

Assuming weak ion cyclotron damping, we include the kinetic effects
 only along the longitudinal (x) direction. Let the ion distribution function
 $F(x, t, \mathbf{v})$ be separated into the longitudinal and perpendicular directions as
 follows

$$F(x, t, \mathbf{v}) = f(t, x, v_x)g(t, x, v_y, v_z), \quad (1)$$

67 the Vlasov - Hall -MHD equations are obtained as follows (Araneda, 1998;
 68 Nariyuki and Hada, 2006; 2007)

$$\frac{\partial f}{\partial t} = -v_x \frac{\partial f}{\partial x} + \frac{1}{\rho} \frac{\partial}{\partial x} \left(T_e \rho + \frac{|b_\perp|^2}{2} \right) \frac{\partial f}{\partial v_x}, \quad (2)$$

$$\frac{\partial u_\perp}{\partial t} = -u_x \frac{\partial u_\perp}{\partial x} + \frac{1}{\rho} \frac{\partial b_\perp}{\partial x}, \quad (3)$$

$$\frac{\partial b_\perp}{\partial t} = \frac{\partial}{\partial x} \left(u_\perp - u_x b_\perp - \frac{i}{\rho} \frac{\partial b_\perp}{\partial x} \right). \quad (4)$$

69 where ρ is the plasma density (quasi-neutrality assumed), u_x is the longitudi-
 70 nal bulk velocity, $b_\perp = b_y + ib_z$ and $u_\perp = u_y + iu_z$ are the complex transverse
 71 magnetic field and bulk velocity, and e_x is the longitudinal electric field,
 72

73 respectively. All the normalizations have been made using the background
 74 constant magnetic field, density, Alfvén velocity, and the ion gyro-frequency.

75 The total pressure is given as $p = p_e + p_i$, where p_e and p_i are electron
 76 and ion (proton) pressure, respectively. In the present study, isothermal
 77 electrons are assumed ($p_e = T_e \rho$) (, namely, the total energy in the system
 78 is not conserved). It is also assumed that the ion and electron pressures are
 79 isotropic.

80 In this study, we solve the Vlasov equation (2) with the time-advance
 81 algorithm called “splitting method” (Cheng and Knorr, 1976), in which the
 82 Vlasov equation (2) is split into the following two advection equations:

$$\frac{\partial f}{\partial t} = -v_x \frac{\partial f}{\partial x} \quad (5)$$

$$\frac{\partial f}{\partial t} = \frac{1}{\rho} \frac{\partial}{\partial x} \left(T_e \rho + \frac{|b_\perp|^2}{2} \right) \frac{\partial f}{\partial v_x}. \quad (6)$$

83 The splitting scheme is widely used because of its simplicity of the algorithms
 84 and ease of programming. The time advance of distribution function $f(x, v_x)$
 85 is first carried out by shifting the distribution function in the x direction (5)
 86 with the time step $\Delta t/2$, shifting the distribution function in the v_x direction
 87 (6) with the time step Δt and again shifting the distribution function in the x
 88 direction (5) with the time step $\Delta t/2$. The spatial profiles of plasma density
 89 ρ is computed by integrating the distribution function over v_x . In parallel
 90 with solving the Vlasov equation, the transverse momentum equation (3) and
 91 the induction equation (4) are solved by the rational Runge-Kutta scheme for
 92 time integration and the spectral method for evaluating spatial derivatives.
 93 The number of cells is $1024 \sim 2048$ in the x direction and is 600 in the v_x
 94 direction over a velocity range from $v_{max} = 2.4$ to $v_{min} = -2.4$. The grid
 95 spacing is equal to $\Delta x = 0.25$, and the time step is equal to $\Delta t = 0.01$.
 96 The boundary condition is periodic for the configuration space and the free
 97 boundary for velocity space. We adopt PIC scheme (Positive Interpolation
 98 for hyperbolic Conservation laws) suggested by Umeda (Umeda, 2008) for
 99 time advancement of the Vlasov equation.

100 To analyze the parametric instability of Alfvén waves, we give monochro-
 101 matic, circular polarized and parallel propagating parent waves as initial
 102 conditions. The initial Alfvén wave is written as $b_\perp = b_0 \exp(-ik_0 x)$, $u_\perp =$
 103 $u_0 \exp(-ik_0 x)$, where b_0 is the amplitude of parent Alfvén waves, $u_0 =$
 104 $-b_0/v_{\phi 0}$ (Walen relation), where the phase velocity $v_{\phi 0} = \omega_0/k_0 (> 0)$, $\omega_0^2 =$

105 $k_0^2(1 + \omega_0)$. We adopt the notation that the positive and negative ω_0 cor-
 106 responds to the right hand polarized (RH-) and left hand polarized (LH-)
 107 waves. The plasma density is $\rho = \rho_0 = 1$, $u_x = u_{x0} = 0$, and $f = f_0$
 108 is given by the isotropic Maxwellian distribution function. Superposed with
 109 the parent wave is a small amplitude white noise with $\langle |\rho_{noise}|^2 \rangle^{1/2} = 10^{-5}$.

110 In the present paper, the ion hybrid simulations are also performed in a
 111 way very similar to that described in Nariyuki *et. al.*(2007) to compare the
 112 results with those obtained by the Vlasov-MHD simulation.

113 3. Simulation results

114 We first show the simulation results (Run 1) of the parametric instabil-
 115 ity of circularly polarized Alfvén waves with $k_0 = -0.4049$, $b_0 = 0.25$, and
 116 $\beta_i = 0.07$, $\beta_e = 0.5$, which parameters are same as those in Araneda *et.*
 117 *al.*(2008). With these parameters, the modulational instabilities are dom-
 118 inant (Araneda *et. al.*, 2008). Figure 1(a) shows the snapshot of the ion
 119 distribution at $t = 1000$, when the instability is almost saturated. Same
 120 as the ion hybrid simulation in Araneda *et. al.*(2008), ions trapped by the
 121 nonlinear density fluctuations are observed. Figure. 1(b) shows the scatter
 122 plot of the ion hybrid simulation plotted in the $x - v_x$ phase space at $t = 620$,
 123 which corresponds to the Fig. 4(c) in Araneda *et. al.*(2008).

124 Figure. 2 shows the wave power history of the wave mode with the max-
 125 imum growth rates in the Vlasiv-MHD simulation and ion hybrid simula-
 126 tion, respectovely. The linear growth of the Vlasiv-MHD simulation agree
 127 well with the those in the linear analysis, which maxmum growth rate is
 128 0.0141. Furthermore, since the initial parent Alfvén wave is weakly nonlin-
 129 ear ($b_0^2 = 0.0625$), the linear growths of the ion hybrid simulation agree with
 130 the linear growth of Vlasiv-MHD simulation as expected by the results in
 131 the past studies (Bugnon *et. al.*, 2004; Nariyuki and Hada, 2007). The dif-
 132 ference of the wave power at early time is due to the numerical noise of the
 133 ion hybrid simulation, which uses the super-particles.

134 Figure. 3 shows the time evolution of the magnetic field (b_\perp) power spec-
 135 trum, plotted in the phase space of the wave number (k) and time, in the
 136 Vlasov-MHD simulation and the ion hybrid simulation, respectively. While
 137 the modulational instability (around $k \sim -0.2$ and -0.6) are very similar,
 138 the daughter waves related to the secondary decay instability (wave excita-
 139 tion at $k > 0$) are excited at the different wave number (around $k \sim 0.1$ in
 140 the Vlasov-MHD simulation and $k \sim 0.05$ in the ion hybrid simulation). It

141 is worth noting that while the assumptions in the Vlasov-MHD simulations
 142 are thought to be the main cause of such a difference, numerical noises in
 143 the ion hybrid simulations possibly influence the resulting plasma conditions
 144 at the nonlinear stage, since these also influence the parametric instabilities
 145 themselves. Thus, the extended Vlasov-MHD simulation and the full-Vlasov
 146 simulation are necessary to clarify the cause of such differences.

147 As a matter of fact, the Vlasov-MHD system corresponds exactly with the
 148 full-Vlasov system (the system of ion hybrid simulations) under the “static
 149 approximation” $\rho \propto |b|^2$ (Mjølhus, 1976; Mjølhus and Wyller, 1988), which is
 150 consistent with the condition that parallel electric field (E_x) is the potential
 151 force and the plasmas are isothermal. We here emphasize that in spite of a
 152 lot of assumptions, as far as the nonlinearity in the system is not so large,
 153 the present Vlasov-MHD simulation model validly solves time evolution of
 154 the Alfvén waves both in the linear and nonlinear stage.

155 We finally mention about the simulation results (Run 2) of the parametric
 156 instability of circularly polarized Alfvén waves with $k_0 = 0.196$, $b_0 = 0.4$, and
 157 $\beta_i = 0.01$, $\beta_e = 0.32$. The decay instability is dominant with these parame-
 158 ters (see Nariyuki and Hada, 2007). Figure 4 shows the wave power history
 159 of the wave mode with the maximum growth rates in the Vlasov-MHD sim-
 160 ulation (black lines) and ion hybrid simulation (gray lines). In contrast to
 161 the previous run, since the amplitude of the initial parent wave is relatively
 162 large ($b_0^2 = 0.16$), the linear growth rates of the Vlasov-MHD system disagree
 163 with the ion hybrid simulation (Nariyuki and Hada, 2007). At the nonlinear
 164 stage, the backward acceleration is caused by the steepen wave packets of ex-
 165 cited daughter Alfvén waves in the Vlasov-MHD simulations (Fig. 5(a)). We
 166 remark that such an acceleration is hardly observed in the present ion hybrid
 167 simulation (Fig. 5(b)). It is because that since the number of accelerated
 168 particle is very small, the number of particles (1500 per cell in the present
 169 simulation), which is not smaller than that in the past studies, is insufficient
 170 to clarify the acceleration.

171 Actually, as shown in Fig. 4, the results of Vlasov-MHD simulations are
 172 not valid when the amplitude of the parent Alfvén waves are relatively large.
 173 On the other hand, we infer that such a backward acceleration *can* occur
 174 in the full Vlasov system. Of course, it does not ensure the quantitative
 175 validity of the Vlasov-MHD model. We believe that the Vlasov-MHD model
 176 can make the suggestions to the ion hybrid simulation, which usually need
 177 much more computational load than the Vlasov-MHD model due to use of

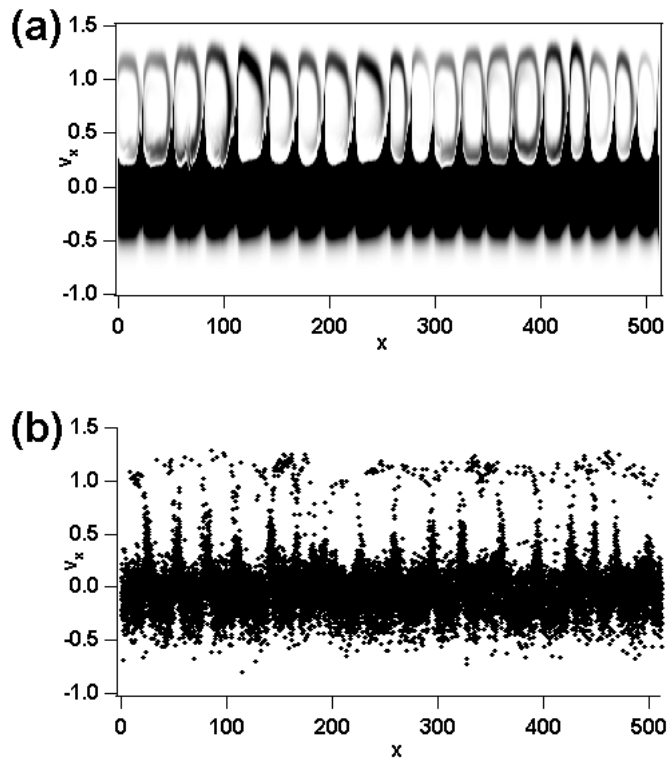


Figure 1: (a)The ion distribution function of the Vlasov-MHD simulation plotted in the $x - v_x$ phase space at $t = 1000$ (Run 1). (b)The scatter plots of the ion hybrid simulation plotted in the $x - v_x$ phase space at $t = 620$.

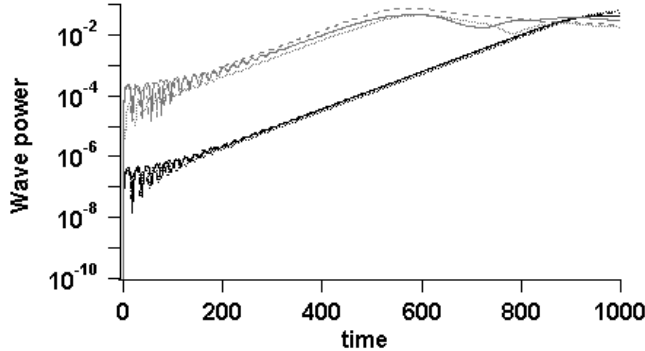


Figure 2: Wave power history of the wave mode with the maximum growth rates in the Vlasiv-MHD simulation (black lines) and ion hybrid simulation (gray lines). The solid, dotted and dashed lines indicate the wave power history of the wave mode with $k = -0.1593$, $k = -0.1718$, $k = -0.1847$, respectively. The growth rates (wave number) measured in the Vlasiv-MHD simulation are 0.01395 ($k = -0.1593$), 0.01385 ($k = -0.1718$), and 0.01388 ($k = -0.1847$). Those measured in the ion hybrid simulation are 0.01287 ($k = -0.1593$), 0.01352 ($k = -0.1718$), 0.014 ($k = -0.1847$), which are very similar to those in Araneda *et. al.*(2008).

178 the large number of particles.

179 4. Conclusion and Discussion

180 In the present paper, we discussed the nonlinear evolution of finite ampli-
 181 tude Alfvén waves using the Vlasov-MHD simulation code, which is a gener-
 182 alized Landau fluid model including the nonlinear wave-particle interactions.
 183 It was confirmed that while the Landau damping should be evaluated along
 184 perturbed field lines (Finn and Gerwin, 1996), as far as the nonlinearity of
 185 parent Alfvén waves are weak, numerical results of the present Vlasov-MHD
 186 simulation agree well with those of the ion hybrid simulations both in the
 187 linear and nonlinear stage. It is worth noting that while the computational
 188 load of Vlasov-MHD code is much less than that of ion hybrid simulation.
 189 On the other hand, when the nonlinearity of parent Alfvén waves are not
 190 weak, the present Vlasov-MHD simulation is not proper. Furthermore, the
 191 Vlasov-MHD model is also inadequate for the high ion beta plasmas, since
 192 the finite Larmor radius effects are neglected.

193 We note that in spite of restriction on nonlinearity and ion kinetics, the
 194 present Vlasov-MHD model can be applied to several heliospheric problems.

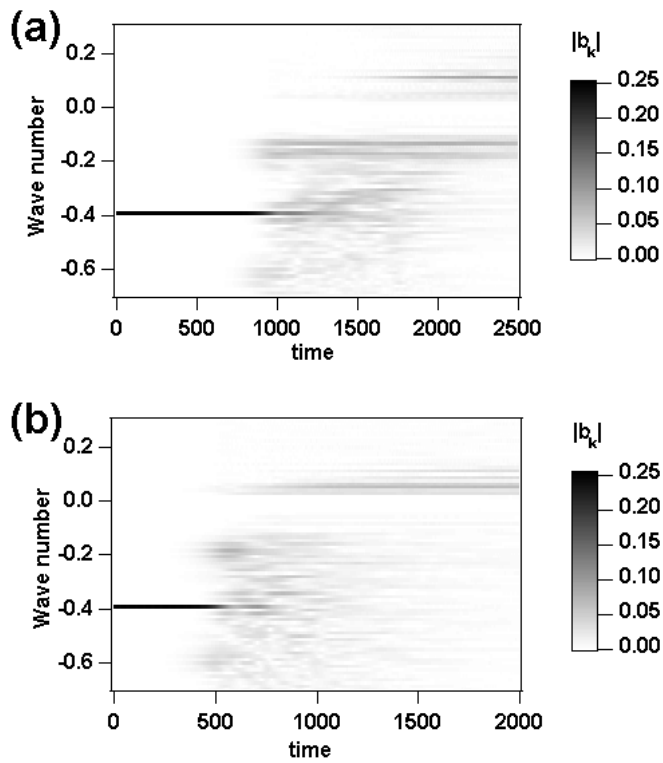


Figure 3: Time evolution of the magnetic field (b_{\perp}) power spectrum, plotted in the phase space of the wave number (k) and time, in (a) the Vlasov-MHD simulation and (b) the ion hybrid simulation.

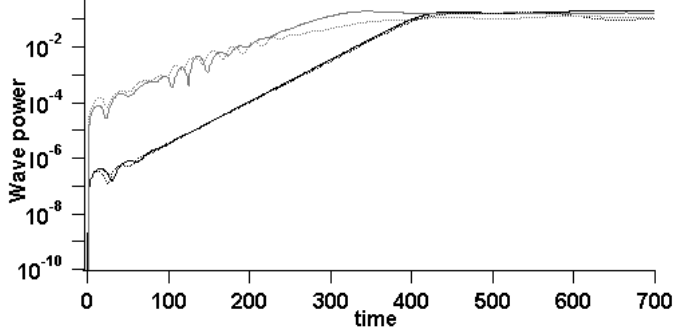


Figure 4: Wave power history of the wave mode with the maximum growth rates in the Vlasiv-MHD simulation (black lines) and ion hybrid simulation (gray lines). The solid and dotted lines indicate the wave power history of the wave mode with $k = -0.098172$, $k = -0.12271$, $k = -0.1847$, respectively. The growth rates (wave number) measured in the Vlasiv-MHD simulation are 0.0344 ($k = -0.098172$) and 0.0339 ($k = -0.12271$). Those measured in the ion hybrid simulation are 0.0262 ($k = -0.098172$) and ~ 0.0243 ($k = -0.12271$).

195 One of them is the solar coronal heating / solar wind acceleration by Alfvén
 196 waves propagating from the photosphere (Suzuki and Inutsuka, 2006). Since
 197 the amplitude of the magnetic fluctuations is not so large and the beta ratio
 198 is small (Suzuki and Inutsuka, 2006; Tanaka *et. al.*, 2007), the assumption
 199 in the Vlasov-MHD system is well satisfied.

200 The characteristics of the observed velocity distribution function near the
 201 sun (*e.g.* Marsch, 2006) is one of the important constraint on the solar coronal
 202 heating and solar wind acceleration model. Namely, the generation processes
 203 of the heliospheric nonequilibrium plasmas such as ion beam components,
 204 temperature anisotropy, and the relative speed among the ion species should
 205 be comprehensively examined in the model. We note that such a point of
 206 view is important for the collaborating works among future missions (Bepi-
 207 Colombo, SCOPE/Cross-Scale, Solar-C, Solar Orbiter, and so on), which
 208 achievements will contribute toward the heliospheric science.

209 Acknowledgement

210 This work was supported by Grant-in-Aid for Young Scientists (Start-
 211 up) No.20840042 (Y. N.) from JSPS and Grant-in-Aid for Young Scientists
 212 (B) No.21740352 (T. U.) from MEXT of Japan. The hybrid simulation code

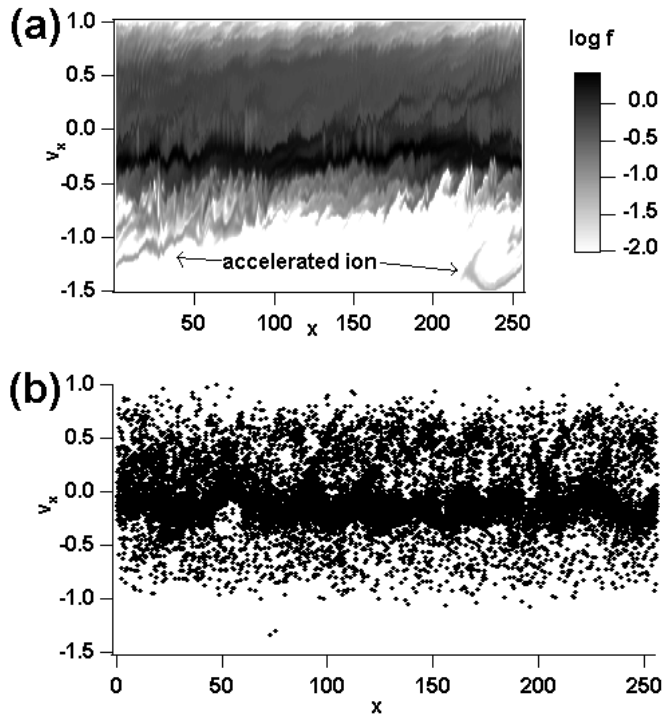


Figure 5: (a)The ion distribution function of the Vlasov-MHD simulation plotted in the $x - v_x$ phase space at $t = 1000$ (Run 2). (b)The scatter plots of the ion hybrid simulation plotted in the $x - v_x$ phase space at $t = 800$. In the present paper, 25,000 particles (1/200 of the total particles) are plotted.

213 was kindly provided by Dr. K. Tsubouchi, and the simulation run was per-
214 formed with the KDK system of the Research Institute for Sustainable Hu-
215 manosphere (RISH) at Kyoto University as a collaborative research project.

216 **References**

- 217 [1] Araneda, J. A.: Parametric instabilities of parallel propagating Alfvén
218 waves: Kinetic effects in the MHD-model, *Phys. Scr.*, T75, 164.
- 219 [2] Araneda, J. A., Marsch, E., Vinas, A. F., 2007. Collisionless damping of
220 parametrically unstable Alfvén waves, *J. Geophys. Res.*, 112, A04104.
- 221 [3] Araneda, J. A., Marsch, E., Vinas, A. F., 2008. Proton core heating
222 and beam formation via parametrically unstable Alfvén-cyclotron waves,
223 *Phys. Rev. Lett.*, 100, 125003.
- 224 [4] Bugnon, G., Passot, T., Sulem, P. L., 2004. Landau-fluid simulations of
225 Alfvén-wave instabilities in a warm collisionless plasma, *Nonl. Proc. in*
226 *Geophys.*, 11, 609.
- 227 [5] Champeaux, S., Laveder, D., Passot, T., Sulem, P. L., 1999. Remarks
228 on the parallel propagation of small-amplitude dispersive Alfvén waves,
229 *Nonl. Proc. in Geophys.*, 6, 169.
- 230 [6] Cheng, C.Z., Knorr, G., 1976. The integration of the Vlasov equation in
231 configuration space, *J. Comp. Phys.*, 22, 330.
- 232 [7] Daughton, W., Gary, S. P., 1998. Electromagnetic proton/proton insta-
233 bilities in the solar wind, *J. Geophys. Res.*, 103, 20613.
- 234 [8] Finn, J. M., Gerwin, R. A., 1996. Parallel transport in ideal magneto-
235 hydrodynamics and applications to resistive wall modes, *Phys. Plasmas*,
236 3(6), 2469-2471.
- 237 [9] Hamilton, K., Smith, C. W. Vasquez, B. J., Leamon, R. J., 2008.
238 Anisotropies and helicities in the solar wind inertial and dissipation
239 ranges at 1 AU, *J. Geophys. Res.*, 113, A01106.
- 240 [10] Kumashiro, T., Hada, T., Nariyuki, Y., Umeda, T., Vlasov simulation
241 of finite amplitude magnetohydrodynamic waves in the solar wind: De-
242 velopment of Vlasov-Hall-MHD code, *J. Plasma and Fusion Res. Series*,
243 in press.

- 244 [11] Leamon, R. J., Smith, C. W., Ness, N. F., Matthaeus, W. H., 1998. Ob-
245 servational constraints on the dynamics of the interplanetary magnetic
246 field dissipation range, *J. Geophys. Res.*, 103, 4775.
- 247 [12] Lin, C. C., Tsai, C. L., Chen, H. J., Weng, C. J., Chao, J. K., Lee, L.
248 C., 2009. A possible generation mechanism of interplanetary rotational
249 discontinuities, *J. Geophys. Res.*, 114, A08102.
- 250 [13] Marsch, E., Muhlhauser, K. H., Schwenn, R., Rosenbauer, H., Pilipp,
251 W., Neubauer, F. M., 1982, Solar wind protons: Three-dimensional
252 velocity distributions and derived plasma parameters measured between
253 0.3 and 1 AU, *J. Geophys. Res.*, 87(A1), 52.
- 254 [14] Marsch, E., 2006. Kinetic Physics of the Solar Corona and
255 Solar Wind, *Living Rev. Solar Phys.*, 3(1). [Online Article],
256 <http://www.livingreviews.org/lrsp-2006-1>
- 257 [15] Mjølhus, E., 1976. On the modulational instability of hydromagnetic
258 waves parallel to the magnetic field, *J. Plasma. Phys.*, 16, 321.
- 259 [16] Mjølhus, E. and Wyller, J., 1988. Nonlinear Alfvén waves in a finite beta
260 plasma, *J. Plasma Phys.*, 40, 299.
- 261 [17] Mjølhus, E., Hada, T., 1990. Oblique stability of circularly polarized
262 MHD waves, *J. Plasma Phys.*, 43, 257.
- 263 [18] Nakamizo, A., Tanaka, T., Kubo, Y., Shimazu, H., Shinagawa, H., 2009.
264 Development of the 3-D MHD model of the solar corona-solar wind com-
265 bining system, *J. Geophys. Res.*, 114, A07109.
- 266 [19] Nariyuki, Y., Hada, T., 2006. Kinetically modified parametric insta-
267 bilities of circularly-polarized Alfvén waves: Ion kinetic effects, *Phys.*
268 *Plasmas*, 13, 124501.
- 269 [20] Nariyuki, Y., Hada, T., 2007, Consequences of finite ion temperature
270 effects on parametric instabilities of circularly polarized Alfvén waves,
271 *J. Geophys. Res.*, 112, A10107.
- 272 [21] Nariyuki, Y., Hada, T., Tsubouchi, K., 2007. Parametric instabilities of
273 parallel propagating incoherent Alfvén waves in a finite ion beta plasma,
274 *Phys. Plasmas*, 14, 122110.

- 275 [22] Nariyuki, Y., Hada, T., Tsubouchi, K., 2009. Parametric instabilities
276 of circularly polarized Alfvén waves in plasmas with beam protons, *J.*
277 *Geophys. Res.*, 114, A07102.
- 278 [23] Passot, T., Sulem, P. L., 2003. Long-Alfvén wave trains in collisionless
279 plasmas. 2. A Landau fluid approach, *Phys. Plasmas*, 10(10), 3906.
- 280 [24] Passot, T., Sulem, P. L., 2004. A Landau fluid model for dispersive
281 magnetohydrodynamics, *Phys. Plasmas*, 11(11), 5173.
- 282 [25] Suzuki, T. K. and Inutsuka, S., 2005. Making the corona and the fast
283 solar wind: A self-consistent simulation for the low-frequency Alfvén
284 waves from the photosphere to 0.3 Au, *Astrophys. J.*, 632(1), L49.
- 285 [26] Suzuki, T. K. and Inutsuka, S., 2006. Solar winds driven by nonlinear
286 low-frequency Alfvén waves from the photosphere: Parametric study for
287 fast/slow winds and disappearance of solar winds, *J. Geophys. Res.*, 111,
288 A06101.
- 289 [27] Suzuki, T. K., 2008. Coronal heating and wind acceleration by nonlinear
290 Alfvén waves global simulations with gravity, radiation, and conduction,
291 *Nonlin. Processes Geophys.*, 15, 295-304.
- 292 [28] Tanaka, S., Ogino, T. and Umeda, T., 2007. Parametric decay of cir-
293 cularly polarized Alfvén waves in the radially expanding solar wind, *J.*
294 *Geophys. Res.*, 112, A10110.
- 295 [29] Tsiklauri, D., Sakai, J. I., Saito, S., 2005. Phase mixing of shear Alfvén
296 waves as a new mechanism for electron acceleration in collisionless, ki-
297 netic plasmas, *New journal of Phys.*, 7, 79.
- 298 [30] Tsurutani, B. T., Lakhina, G. S., Pickett, J. S., Guarnieri, F. L., Lin, N.,
299 Goldstein, B. E., 2005. Nonlinear Alfvén waves , discontinuities, proton
300 perpendicular acceleration, and magnetic holes/decreases in interplane-
301 tary space and the magnetosphere: intermediate shock?, *Nonl. Proc. in*
302 *Geophys.*, 12, 321.
- 303 [31] Umeda, T., 2008. A conservative and non-oscillatory scheme for Vlasov
304 code simulations, *Earth Planets Space*, 60(7), 773-779.

- 305 [32] Valentini, F., Veltri, P., Califano, F., Mangeney, A., 2008. Cross-scale
306 effects in solar-wind turbulence, *Phys. Rev. Lett.*, 101, 025006.
- 307 [33] Wu, C. S., Yoon, P. H., 2007. Proton heating via nonresonant scattering
308 off intrinsic Alfvénic turbulence, *Phys. Rev. Lett.*, 99, 075001.
- 309 [34] Yin, L., Winske, D., Daughton, W., Bowersc, K. J., 2007. Kinetic Alfvén
310 waves and electron physics. I. Generation from ion-ion streaming, *Phys.*
311 *Plasmas*, 14, 062104.